Electro-orientation of ellipsoidal erythrocytes

Theory and experiment

Ruth Douglas Miller and Thomas B. Jones
Department of Electrical Engineering, University of Rochester, Rochester, New York 14627 USA

ABSTRACT The frequency-dependent orientation of human and llama erythrocytes suspended in isotonic solutions and subjected to linearly polarized electric fields is examined. Human erythrocytes may be represented as oblate spheroids (3.9:3.9:1.1 μm) with two distinguishable orientations, while the llama cells are approximated as ellipsoids with three distinct axes (4.0:2.0:1.1 μm). Under appropriate experimental conditions, both orientations of the human cells and all three orientations of the llama cells are observed. A theoretical cell model which accounts for the membrane as a thin confocal layer of ideal capacitance is used to predict the orientational spectra. The predicted spectra compare favorably in frequency range and orientational sequence with experimental data. Estimates for cell internal conductivity and permittivity are obtained by adjusting the values of these important parameters to achieve the closest fit of the theoretical curves to the data. By the use of this method, the internal conductivity of llama erythrocytes is estimated to be 0.26 S/m (±20%), while the effective internal dielectric constant and conductivity of *Euglena gracilis* are estimated to be 120 (±10%) and 0.43 S/m (±20%), respectively.

INTRODUCTION

Frequency-dependent orientation of cells was first observed with various protists, erythrocytes, and bacteria (1). Quantitative observations of orientation versus frequency were made by Griffin (2) on erythrocytes, Griffin and Stowell (3) and Ascoli et al. (4) on *Euglena,* and Iglesias et al. (5) on yeast cells. Fomchenkov and Gavrilyuk (6, 7) studied both bacteria (*E. coli*) and human erythrocytes. All of the cells studied were ellipsoidal or spheroidal in outline and oriented their short axes parallel to an applied electric field over some range of frequency. No effort was made to distinguish three orientations of those cells which were ellipsoidal (2).

Several papers utilized a predictive theory for the orientational phenomenon based on an energy minimization argument (8, 9), accounting for the β dispersion of cell membranes (10) by modelling the cell as a lossy dielectric ellipsoid with a thin, insulating outer layer. This theory was compared to experimental data by several workers (4, 11) with some success, despite the objection that such energy arguments are invalid in dissipative media (12, 13). A second theory of orientation (14) derived the torque on a particle from the effective dipole moment induced by the applied electric field. Fomchenkov et al. (15) used Gruzdev's theory quite successfully to determine stable orientation of *E. coli* at a single medium conductivity, including the cell β dispersion explicitly as formulated by Schwan (10).

In the present work the effective moment-based theory is extended to orientation spectra of human and llama erythrocytes and the predictions are compared to experiment over a range of medium conductivities. Orientation spectra of both cell types are obtained by experiment and for the first time all three possible orientations of ellipsoidal cells (llama erythrocytes in this case) are distinguished. For the theoretical comparison, the cells are modeled as layered ellipsoids, including the membrane (β) relaxation implicitly rather than explicitly as in (15). The effective-moment-based model of frequency-dependent orientation is shown to be successful in estimating the internal electrical properties of cells.

Address correspondence to Dr. Ruth Douglas Miller, Department of Electrical and Computer Engineering, Kansas State University, Manhattan, KS 66506-5105, USA.

MATERIALS AND METHODS

Human blood samples obtained from several subjects were treated with sodium citrate to prevent clotting, while the llama blood samples from animals at Seneca Park Zoo, Rochester, NY were treated with potassium EDTA. The human erythrocytes were biconcave disks, with semiaxes averaging 3.9:3.9:1.1 ± 0.2 μm. The length of the shortest axis was measured across the wider, edge region of the cells; the actual width across the "dimpled" region would of course be less. The llama erythrocytes, chosen because of their approximate ellipsoidal shape and uniform interior composition, had semiaxes of 4.0:2.0:1.1 ± 0.2 μm, and were also biconcave, having "dimples" on the sides perpendicular to their shortest axes. Again the thickness of these cells measured through the "dimples" is less than the measured short axis. Cells of both types were suspended in isotonic solutions of calcium chloride (1.2% by weight) and sucrose (9.9% by weight), mixed in varying proportions to obtain suspending media of different conductivities. To 4.3 ml, of each suspending medium one drop of blood was added, and the conductivities of the resulting solutions were measured at 20 kHz, 1 MHz and 10 MHz. The average conductivity was used in plotting the data. Standard deviations were 30% at the lowest conductivity and 15% for all the others. The greater uncertainty at the lowest conductivity is to be expected for solutions near the low end of the multimeter's range.

The orientation chamber, constructed after that in (2), is illustrated in Fig. 1. A microscope slide with a 0.5 mm deep depression fits in the center of the chamber. The platinum wire electrodes, 0.13 mm in diameter, stretch across the slide, suspended above the depression, between screws on one side of the chamber and springs on the other. The screws maintain wire tension, while notches in the chamber sides determine the electrode spacing (about 0.5 mm). A few drops of medium with cells were placed on the slide depression and a coverslip added. With a microscope focused on the plane of the electrodes, cells could be observed clearly only in the region of most uniform field, free of edge effects from the slide and coverslip surfaces. The electric signal was generated by a Fluke 6010A Synthesized Signal Generator (John Fluke

0006-3495/93/05/1588/08 $2.00

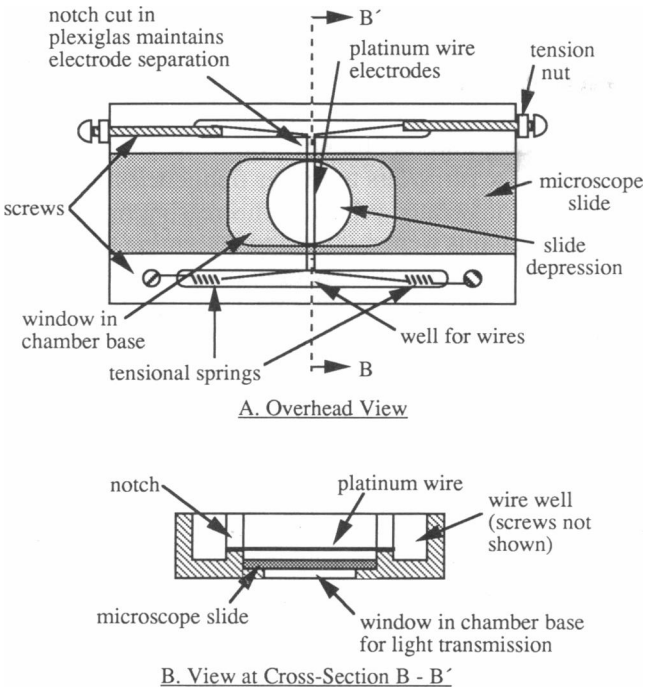

FIGURE 1 (*A*) View of platinum-wired orientation chamber from above. (*B*) Side view of same chamber, at cross-section $B - B'$. Here the window cut in the chamber base can be clearly seen. The wire is shown above the slide surface for clarity; in reality it rests directly on the flat of the slide, and is thus suspended above the slide depression.

Manufacturing Co., Inc., Everett, WA) for frequencies up to 10 MHz and by an HP 608C VHF Signal Generator for frequencies from 10 to 220 MHz. Amplification up to approximately 20 V rms was provided by an IFI 402 Wideband Laboratory Amplifier (IFI Corporation, Ronkonkoma, NY); voltage could not be measured above 10 MHz, the limit of the multimeter. Observations were made with a light microscope.

During the course of each experiment, the orientation chamber was filled and the electric field applied at one frequency (usually either 1 or 220 MHz), with a field strength just sufficient to orient all the cells. The frequency was then changed by steps and the cells' orientations noted at each step. At least two runs were made at each medium conductivity, and the results were found to differ very little from sample to sample.

EXPERIMENTAL RESULTS

Orientation observations

The results of the experiments with human and llama erythrocytes are summarized in Figs. 2 and 3, respectively. Symbols indicate frequencies where orientational preference was noted. Results in Fig. 2 are from two experiments done on different days with different blood samples; those in Fig. 3 are from four different trials. Points are shown side-by-side only near transitions and where results differed. Two orientations of the human cells were distinguishable (the *a* and *b* axes are identical), while three unique orientations of the llama cells were noted. Although not shown in the figures, observations of both cell species were made at frequencies down to 10 Hz; only parallel or *a* orientation was observed below 1 MHz. At some frequencies, no dominant orientation could be distinguished; for example, where "mixed" orientation is indicated, some cells oriented in one direction, others in another; however, no cells were observed that showed no preferred position. On the other hand, "uncertain" orientation indicates that many cells showed no response to the field at all, suggesting that the electrically induced torque was very weak. The vertical bars in Fig. 2 are data from (2) for human erythrocytes suspended in glucose/NaCl medium, and indicate the observed region of mixed orientation, with *a*/*b* orientation below and *c* above. The squares mark the frequencies at which approximately 90% of the cells oriented the same way. Note the general agreement between his data and those of this work, further confirming his observation that the orientation spectra are insensitive to the salt used in the medium. Only one change in orientation ("turnover") was observed by Griffin over the range DC to 400 MHz; the signal generator available for the present study was limited to 220 MHz and below.

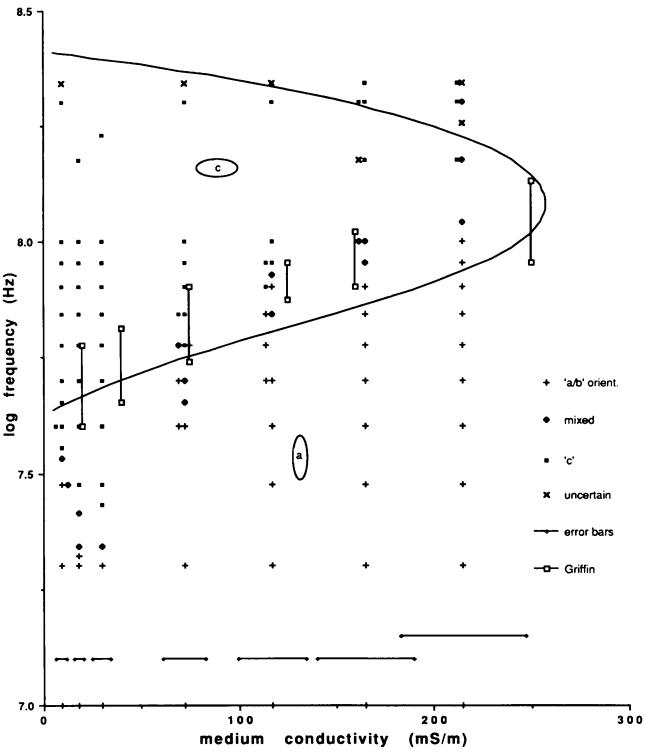

FIGURE 2 Orientational spectra of human erythrocytes in isotonic solutions of sucrose and $CaCl_2$ in varying ratio. Solid lines indicate theoretical turnover frequencies, calculated using the confocal model and the following fluid and particle electrical parameters (from Pauly and Schwan, 1966): $\epsilon_1 = 80\epsilon_0$, σ_1 varied as shown, $\epsilon_2 = 50\epsilon_0$, $\sigma_2 = 0.5$ S/m, $\epsilon_m = 10\epsilon_0$, $\sigma_m = 0.0$, membrane thickness on *y* axis 0.01 μm. Symbols indicate frequencies where orientational preference was noted experimentally. Vertical bars are data from (2); horizontal bars near the *x*-axis indicate the variation in the measured values of medium conductivity.

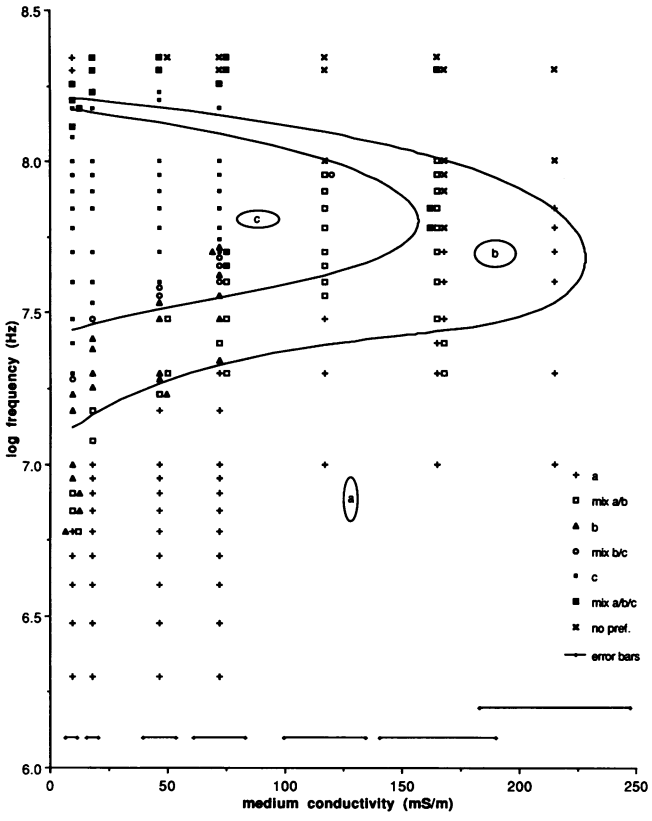

FIGURE 3 Orientational spectra of llama erythrocytes in isotonic solutions of sucrose and $CaCl_2$. Solid lines indicate theoretical turnover frequencies, calculated using the confocal model and the following electrical parameters: $\epsilon_1 = 80\epsilon_0$, σ_1 varied as shown, $\epsilon_2 = 52\epsilon_0$, $\sigma_2 = 0.26$ S/m, $\epsilon_m = 10\epsilon_0$, $\sigma_m = 0.0$, membrane thickness on y axis = 0.01 μm. Symbols indicate frequencies where orientational preference was noted experimentally. Horizontal bars near the x-axis indicate the variation in the measured values of medium conductivity.

At higher frequencies and medium conductivities, especially with the llama cells, it became impossible to apply an electric field of magnitude sufficient to orient the cells without also producing excessive joule heating and the accompanying fluid convection, which carried the cells out of view before they could reach a stable orientation. With llama erythrocytes, convection dominated over the orientational torque at 100 MHz for medium conductivity (σ_1) of 117 mS/m, and affected observations at frequencies as low as 60 MHz for $\sigma_1 \geq 165$ mS/m. While present in the experiments with human cells, convection currents were not a problem except for medium conductivity $\sigma_1 = 215$ mS/m; no clear observations could be obtained at higher medium conductivities.

Other observations

Although the orientational spectra were the main focus of this study, a few other electric-field-induced phenomena were observed. In the lower frequency range, where cells always exhibited the *a* orientation, both species of erythrocytes tended to form pearl chains at higher electric field strengths than necessary to confirm orientation. When the first transition frequency was reached, each cell in a chain would re-orient individually, but mutual interactions and/or friction from neighboring cells shifted these turnovers to higher frequencies than those observed for isolated cells. For this reason, observations made on chains were not used to determine transitions. Chains of human erythrocytes in *c* orientation look like stacks of coins and are referred to in the literature as *rouleaux* (16); some excellent photomicrographs of *rouleau* formation may be found in (17, 18). The llama cells also formed chains in *b* orientation, but these were apparently unstable. Cells in this configuration would invariably begin to spin about their longest axes at a field strength only slightly stronger than that necessary to orient them. The spin frequency was dependent on the field strength. At applied-field frequencies just above the *a* to *c* transition, the human erythrocytes would also spin if they were in proximity to each other, and especially if they were in chains. Both cell species always spun about the longest axis perpendicular to the field. This phenomenon, probably akin to the rotation described in (19), produced a "blinking" effect in the *rouleaux*. As interparticle forces and orienting torques grew weaker at higher frequencies, a function of cell dielectric properties, the tendency to form chains diminished. No chains were observed in either cell species at frequencies 10 to 20 MHz above the *a* or *b* to *c* transition.

ANALYSIS OF DATA

Derivation of torque expression

The orientation phenomenon is caused by an electric-field-induced torque acting on a non-spherical particle. This torque can be easily calculated from the effective dipole moment expression for a homogeneous, lossy dielectric ellipsoid (14, 20). To extend this method to erythrocytes, it is essential to account for the β dispersion caused by the capacitive membrane that encloses these cells. This can be done implicitly, by including the β relaxation in the formulation of the cell's dielectric constant (15), or explicitly, as follows. (See reference 21 for details.)

Although erythrocytes have a biconcave shape, as a first approximation a cell can be modeled as a lossy dielectric ellipsoid surrounded by a thin, insulating shell (8, 21, 22), and centered at the origin. Both the inner and outer boundaries of the layer are surfaces of constant ξ in ellipsoidal coordinates. It should be noted here that these surfaces are *confocal*, and as ξ grows large they approach spheres in shape; thus the thickness of the layer is a function of position. Refer to Fig. 4 *A*, where the layer thickness is exaggerated to show the variation with position clearly. This approximation is used to obtain a closed-form solution to the problem, with the assumption that since the cell membrane is thin, the variation in

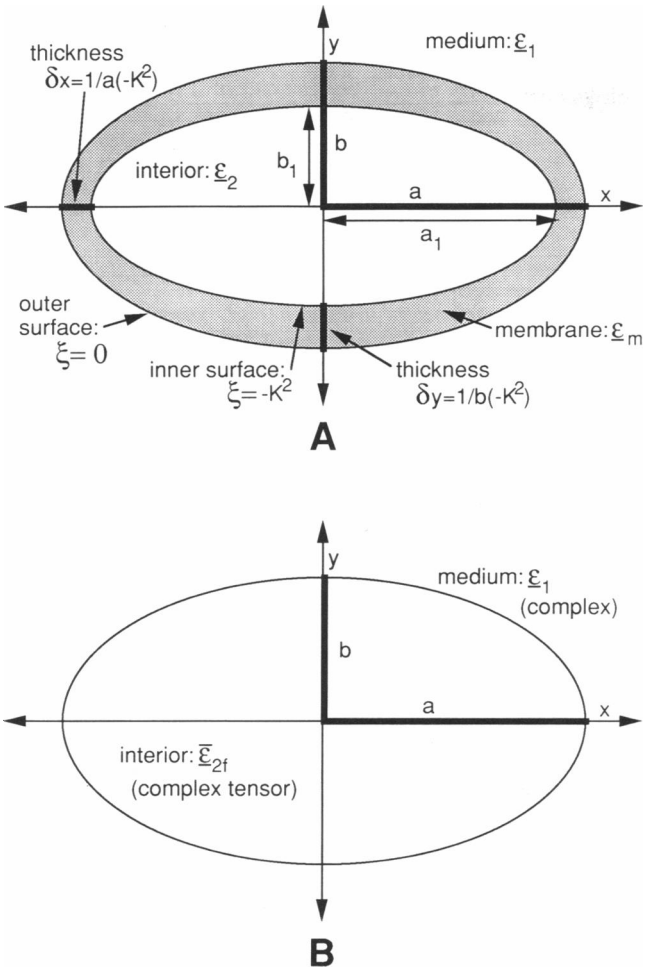

FIGURE 4 (*A*) An ellipsoid with an external, confocal layer of different electrical properties, shown with the shortest (c) axis perpendicular to the page. ϵ = dielectric constant (may be complex). The semiaxes of the external ellipsoid are a, b, and c; a_1, b_1, and c_1 are the semiaxes of the internal ellipsoid; ξ is the coordinate of the ellipsoidal surfaces. The layer thickness, exaggerated for clarity, is specified by the constant K. (*B*) The equivalent homogeneous but anisotropic ellipsoid with tensor permittivity $\underline{\epsilon}_{2f}$, semiaxes a, b, and c. The electric fields around both ellipsoids *A* and *B* are identical.

thickness required by the model will not introduce a large error into the results. Laplace's equation in ellipsoidal coordinates can then be solved for electric potential in the three regions of the cell interior, insulating membrane, and exterior, with boundary conditions that enforce continuity of electric potential and normal flux density at the boundaries between the regions. Finally, the potential in the external medium can be equated with that due to a homogeneous but anisotropic ellipsoid of the same external dimensions, and the resulting equation can be solved for an expression for the homogeneous, anisotropic complex permittivity of the equivalent ellipsoid (Fig. 4 *B*). This method is clearly detailed in (21) and we simply present the final expression for the effective complex anisotropic permittivity of the ellipsoid here:

$$\underline{\epsilon}_{2kf} = \underline{\epsilon}_m \frac{\underline{\epsilon}_m + \nu(\underline{\epsilon}_2 - \underline{\epsilon}_m)(B_{1k} - A_{0k} + 1)}{\underline{\epsilon}_m + \nu(\underline{\epsilon}_2 - \underline{\epsilon}_m)(B_{1k} - A_{0k})} \tag{1}$$

where: $\underline{\epsilon} = \epsilon - j\sigma/\omega$, $\underline{\epsilon}$ is permittivity (F/m), σ conductivity (S/m), ω frequency in rad/s, $j = \sqrt{-1}$, the underline denotes a complex quantity,

$$\nu = \frac{a_1 b_1 c_1}{a_0 b_0 c_0}, \quad B_{1k} = \frac{1}{\nu} A_{1k},$$

$$A_{sk} = \frac{a_s b_s c_s}{2} \int_0^\infty \frac{d\xi}{(t_s^2 + \xi) D_s} \quad \text{and}$$

$$D_s = \sqrt{(\xi + a_s^2)(\xi + b_s^2)(\xi + c_s^2)},$$

$t_s = a_s, b_s, c_s$ for $k = x, y, z$, respectively, and $s = 0, 1$. The integral $B_{1k} - A_{0k}$ may be written:

$$B_{1k} - A_{0k} = \frac{a_0 b_0 c_0}{2} \int_{-K^2}^0 \frac{d\xi}{(t_0^2 + \xi) D_0} \tag{2}$$

where the layer thickness parameter $K^2 = 2a\delta x = 2b\delta y = 2c\delta z$. If the layer is very thin ($K^2 \ll c^2$), then $\nu \approx 1$ and, using the trapezoidal rule, $B_{1k} - A_{0k} \approx K^2/2t_0^2 = \delta t/t_0 = \delta x/a_0$ for $k = x$ and so on. With this change, finally,

$$\underline{\epsilon}_{2kf} = \underline{\epsilon}_m \frac{\underline{\epsilon}_2 + \delta t/t_0(\underline{\epsilon}_2 - \underline{\epsilon}_m)}{\underline{\epsilon}_m + \delta t/t_0(\underline{\epsilon}_2 - \underline{\epsilon}_m)}. \tag{3}$$

To determine stable orientation, the electric-field-induced torque on the ellipsoid is calculated from its dipole moment, the kth component of which is given by (12, 20, 23):

$$\underline{p}_k = \frac{4\pi a_0 b_0 c_0}{3} \epsilon_1 \left[\frac{\underline{\epsilon}_{2k} - \underline{\epsilon}_1}{\underline{\epsilon}_1 + (\underline{\epsilon}_{2k} - \underline{\epsilon}_1) A_{0k}}\right] E_{0k} \tag{4}$$

where E_{0k} is the component of the applied field in the k(x, y, or z) direction. The torque **T** is calculated from:

$$\mathbf{T} = \tfrac{1}{2} \operatorname{Re}[\underline{\mathbf{p}} \times \underline{\mathbf{E}}^*] \tag{5}$$

To determine orientation, only the directions (signs) of the three torque components are needed. The sign of the torque about the z axis is equivalent to that of the frequency-dependent term below:

$$\operatorname{sign}[T_z] = \operatorname{sign}\left\{\operatorname{Re}\left[\frac{\underline{\epsilon}_{2x} - \underline{\epsilon}_1}{\underline{\epsilon}_1 + (\underline{\epsilon}_{2x} - \underline{\epsilon}_1) A_{0x}} - \frac{\underline{\epsilon}_{2y} - \underline{\epsilon}_1}{\underline{\epsilon}_1 + (\underline{\epsilon}_{2y} - \underline{\epsilon}_1) A_{0y}}\right]\right\} \tag{6}$$

and similarly for the other two torque components. For an isotropic ellipsoid, $\underline{\epsilon}_{2x} = \underline{\epsilon}_{2y} = \underline{\epsilon}_{2z}$ and Eq. 6 can be simplified considerably (20). However, as we have seen, the layered ellipsoid cell model leads to an anisotropy in $\underline{\epsilon}_{2k}$ (Eq. 3) and the final expression of Eq. 6 with $\underline{\epsilon}_{2k}$ replaced by $\underline{\epsilon}_{2kf}$ is not apparently factorable. Although attempts to factor Eq. 6 using the computer program MAXSYMA were unsuccessful, its sign is readily calculated for specific cases. The frequencies at which the magnitude of the torque about a non-oriented axis passes through zero are those at which turnovers will

occur. (A change in sign of the torque about the axis parallel to the field will have no effect on orientation.)

Theoretical orientation spectra of erythrocytes and *Euglena gracilis*

The electrical properties of human erythrocytes have been measured as $\epsilon_2 = 50.1 \pm 0.4\epsilon_0$, $\sigma_2 = 0.518 \pm 0.007$ S/m (reference 24). (The permittivity of free space, $\epsilon_0 = 8.854 \cdot 0^{-12}$ F/m.) The electrical properties of cell membranes vary little between species and even between classes (10, 25, 26, 27). A representative value of membrane capacitance per unit area is $C_m = 9$ mF/m^2, (or equivalently, $\epsilon_m = 10\epsilon_0$ and the thickness $\delta t = 100$ Å) and membrane resistance is often negligible. Since the mathematics of the confocal model necessitate a smooth spheroid with a membrane of varying thickness, the erythrocyte semiaxes were assumed to have the lengths given above, and the value of 100 Å was assumed to be that of the membrane on the intermediate (b) axis (equal to the a axis for human erythrocytes). The suspending media have the properties $\epsilon_1 = 80\epsilon_0$ and σ_1 ranging from 9 to 215 mS/m. The orientation spectra delineated by the solid lines in Fig. 2 were calculated using these values in the equivalent equation to Eq. 6 for sign [T_y] and finding the zero crossings of this function. The lines, drawn through theoretical turnover frequencies, delineate the two regions of a/b and c orientation.

Measured electrical properties of llama cells have not been published, so estimates were made of certain parameters with the generally held assumption that these properties do not vary widely between mammalian species. Based upon the findings in (24), we assumed $\epsilon_2 = 52\epsilon_0$. The membrane capacitance was chosen to be the same as that of human erythrocytes, that is, $C_m = 9\ \mu$F/cm^2. The cell shape was assumed to be smoothly ellipsoidal, with dimensions as given above. These choices left only the internal conductivity σ_2 to be determined. The approach taken was to adjust σ_2 to achieve a subjective "best fit" of the theoretical turnover frequency curves to the experimental data. This best fit gave an estimate of $\sigma_2 = 0.26$ S/m. Again the lines in Fig. 3 were calculated using Eq. 6 as well as the corresponding equations for sign [T_y] and sign [T_z], since llama cells have three possible orientations. Uncertainties in solution conductivity measurements as well as the bandwidths of "mixed" orientation project uncertainties of 20% in σ_2 and 10% in ϵ_2.

Fig. 5 shows the experimentally obtained orientation spectra from (4) and (3) for *Euglena gracilis*. The *Euglena* were described in (3) as being 65 μm long, with an axis ratio of 5.4:1:1, and in (4) as having semiaxes measuring 30:5:5 μm, so the assumption of smooth prolate spheroidal shape seems reasonable. Data points surround the region of b/c orientation, and indicate the "average" transition frequencies observed. No perpendicular orientation was observed for medium conductivity greater than 50 mS/m. The various symbols indicate different solution salts as given in the key; note these

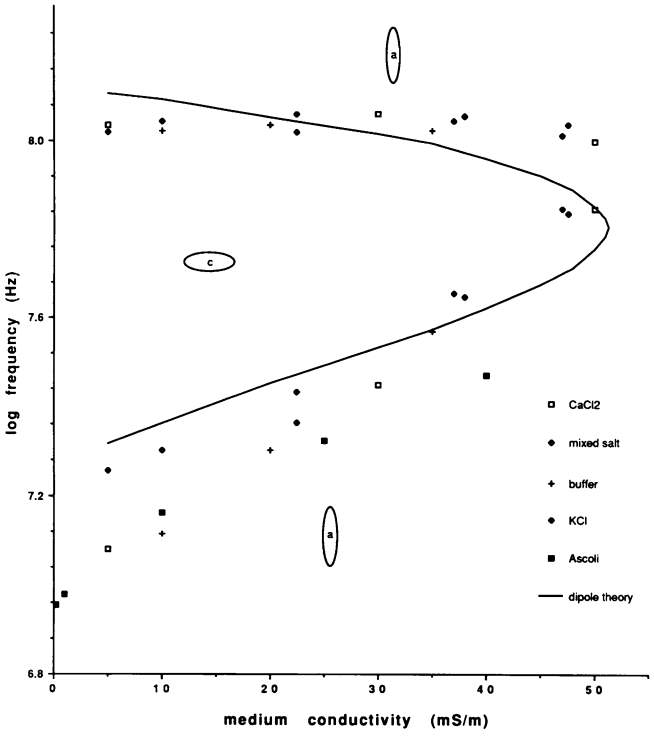

FIGURE 5 Orientational spectra of *Euglena* in various salt solutions, and theoretical predictions from the dipole-based theory. Data points from the following sources: CaCl2: (3), cells in $CaCl_2$ solution; mixed: (3), suspending medium of 10 g NaCl, 10 g $CaCl_2$, 6 g KCl, and 2 g $MgSO_4 \cdot 7H_2O$ each per liter before dilution; buffer: (3), suspending medium KH_2PO_4–KOH buffer, pH 7; KCl: (3), cells in KCl solution; Ascoli: (4), suspending medium composition not given. Solid lines indicate theoretical turnover frequencies calculated using the confocal model with cell and medium properties: $\epsilon_1 = 80\epsilon_0$, $\epsilon_2 = 120\epsilon_0$, $\sigma_2 = 0.43$ S/m, $\epsilon_m = 10\epsilon_0$, and membrane thickness on y and z axes = 0.01 μm. Cell axis ratio 32.5:6.0:6.0 μm.

different salts had no significant effect on orientation. The curve, calculated as for the human and llama erythrocytes, is drawn through theoretical turnover frequencies, and orientation is predicted to be a outside of them and b/c inside. The axis ratio was chosen from (3), and properties of the external medium and cell membrane were fixed. The internal permittivity and conductivity were varied to obtain a subjective best fit with the data. The resulting values of $\epsilon_2 = 120\epsilon_0$ and $\sigma_2 = 0.43$ S/m are the *effective* values for the combination of cytoplasm and intact organelles, as the cell model used assumes the cell interior is homogeneous. These values should not be assumed to relate directly to the actual conductivities and permittivities of the *Euglena* cytoplasm and organelle membranes and interiors; rather a complex relationship along the lines of Eq. 1 should be expected.

DISCUSSION

Human erythrocytes

The predictive success of the orientational theory developed above can be tested by comparing its predictions

with the experimental results for human erythrocytes. The electrical parameters of these cells are known, so that the theoretical spectra calculated using those parameters in Eqs. 3 and 6 should match the experimental spectra if the theory is a reasonable model for this system. As can be seen in Fig. 2, the agreement between theory and experiment is quite good at low frequencies. Heating effects prevented testing of the prediction that no turnovers should occur at conductivities above 250 mS/m; this is in accord with the theory in that the torque is expected to be very small when σ_1 is close to σ_2, so that high voltages are necessary to align cells. Such high voltages also mean increased conduction and thus increased joule heating. The presence of the higher frequency turnover could not be confirmed because of the 220 MHz frequency limit on the signal generator. Griffin (2) performed experiments at frequencies of up to 400 MHz, and reported only the lower turnover, though he did not give detailed descriptions of cell behavior at frequencies above 140 MHz. The theory predicts extremely weak torques at frequencies above that of the high-frequency turnover, so that the "uncertain" orientation seen in this work at high frequencies is expected. Although the correctness of the predicted high-frequency turnover of human erythrocytes cannot be assessed, the low-frequency orientational behavior of these cells is adequately predicted by the effective dipole theory. The model assumptions of smooth spheroidal shape and confocal membrane do not seem to affect the results appreciably.

Llama erythrocytes

Orientation theory provides a means of estimating the unknown cell properties of ϵ_2 and σ_2 from the cells' orientation spectra, and this was done for llama erythrocytes, as illustrated in Fig. 3. Note that the general curve shape and orientation sequence are well matched by the theory; these properties are not affected by changes in ϵ_2 and σ_2. The internal conductivity σ_2 was chosen to match the low-frequency spectra best; note that the high-frequency spectra as well as the results at high σ_1 are also reasonably matched with this approach. Where orientation appeared uncertain, the theory also predicts very weak torques (above the high-frequency turnovers and in media with $\sigma_1 \geq 120$ mS/m). The *b* orientation predicted at high frequencies was not observed, but the frequency band is narrow enough that it could well be obscured by the variability of individual cells. The observation of "mixed *a*/*b*/*c*" orientation suggests this *b* region is indeed present, though possibly at slightly higher frequencies than predicted. Although convective heating interfered with orientation at frequencies above about 60 MHz, only *a* orientation was observed at the highest medium conductivity, consistent with the theory.

There are, however, several discrepancies to be considered. The first turnover is observed in the least conductive solution (σ_1 = 9 mS/m) at a frequency much lower than that predicted. Also in general the higher turnover(s) appear to occur up to 100 MHz above the predicted frequencies. This is quite possibly an experimental artifact of the weak torque and interfering convection currents. As with human erythrocytes, observations at frequencies up to 500 or 1,000 MHz might help to confirm the actual higher turnover frequencies. The approximation introduced by the use of the confocal model to represent the llama cells could also explain the discrepancy between theory and experiment. Modeling the membrane as a dielectric layer of non-uniform thickness slightly exaggerates the differences between the cell axes, and thus changes the widths of the theoretical *b* and *c* orientation regions. Finally, the internal conductivity used in the theoretical cell model (0.26 S/m) is lower than any measured in other erythrocyte species, but σ_2 must be set within the range 0.21–0.31 S/m to match the experimental data. It would be desirable to measure the llama erythrocyte internal electrical properties directly by other means and see if they differ so much from those of related mammals such as cattle and sheep. Unfortunately this measurement could not be done in this study.

Euglena gracilis

The dipole-based orientation theory provides an explanation of the observed orientation phenomena, not only for "simple" cells such as erythrocytes but also for more complicated cells such as *Euglena*. To illustrate this, the data from (3) and (4) are plotted against theoretical turnover spectra in Fig. 5. The values of ϵ_2 and σ_2 were adjusted to obtain a subjective best fit of theory to experiment. Because *Euglena* has a much more complex internal structure than mammalian erythrocytes (28), the values for effective internal permittivity and conductivity should be expected to differ from those of such cells. Its thick, highly convoluted pellicle and its membrane-bounded organelles complicate the cell's electrical behavior. The model used in this paper assumes a homogeneous cell interior, and therefore the values of $\epsilon_2 = 120\epsilon_0$ and $\sigma_2 = 0.43$ S/m predicted by the theory correspond to those of an equivalently sized, smooth, homogeneous particle with a thin insulating outer membrane and the same externally apparent electrical characteristics as a *Euglena*. The protist's internal structure and resultant frequency-dependent effective permittivity and conductivity may account for the difference in shape between the dipole theory prediction and the experimental points of Fig. 5.

Comparison of dipole-based and energy theories

Fig. 6 shows the theoretical orientation spectra of human erythrocytes (as in Fig. 2), along with the orientation spectra predicted using the "energy theory" (9) with same cell properties. Note that according to the energy theory, human erythrocytes, and any other particles with

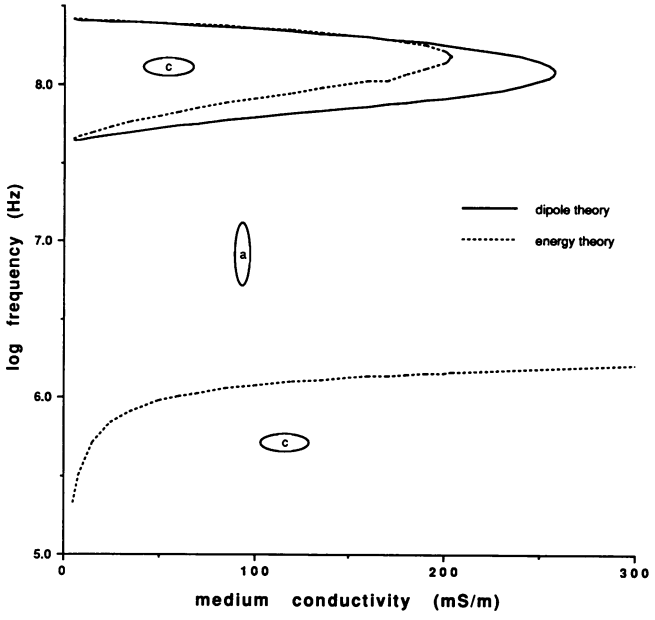

FIGURE 6 Comparison of the orientation spectra, calculated using the dipole and energy theories, for human erythrocytes. Cell and medium properties same as in Fig. 2. The low-frequency region of *c* orientation is predicted only by the energy theory; the dipole theory predicts *a*/*b* orientation down to DC.

thin, insulating outer layers and dimensions typical of biological cells, should orient *c* axis parallel to the applied electric field from DC to the mid-radio-frequency range for any reasonable medium conductivity. The lower curve continues down and intersects DC at zero medium conductivity. This prediction arises from the form of the energy model equations at the low-frequency limit, where particle and medium electrical properties cease to affect torque sign. The experimental observations of this work and others (1–5) plainly contradict this prediction. The differences between the predictions of the potential energy and dipole theories are greatest at low frequencies, and decrease to zero at the high-frequency limit; however, the failure of the potential energy theory at low frequencies, coupled with the objections in (13), suggests the dipole theory provides a better explanation of the orientational phenomenon.

Despite some discrepancies between theory and experiment, the induced dipole theory proves to be a useful predictive tool. The region of turnovers is correctly predicted, as are the turnover sequence and the approximate torque magnitude. The orientational behavior of both the erythrocytes and *Euglena* is adequately explained by the theory, which has proved relatively simple to apply to these cases. Differences in the internal properties of human and llama erythrocytes have been found. These differences should be further examined by other means, and the theory should be extended to other species through more orientation experiments.

CONCLUSIONS

In this paper the dipole-based orientational theory has been expanded to include biological cells, modeled as lossy dielectric particles coated with a thin, insulating layer. The results from this model have been favorably compared with the experimental orientation spectra of human and llama erythrocytes. Evidence has been presented suggesting that llama erythrocytes may have a relatively low internal conductivity (0.26 S/m.) Previously published orientation spectra of *Euglena gracilis* have been used in combination with the dipole-based theory to estimate the effective internal permittivity and conductivity of these protists. The dipole-based theory developed herein provides an adequate explanation of the frequency-dependent orientation of biological cells, and suggests that differences in cell internal electrical properties may be discerned from differences in their orientational spectra. Since many cell types are non-spherical, and since changes in orientation occur over a frequency range useful for observations of cell electroporation and electrofusion (29, 30) there is a need to understand the orientational phenomenon more fully in order to predict orientation changes when manipulating cells with RF electric fields. Also, the electrical properties of cells with complex internal structures (including most cells but erythrocytes) cannot be measured by homogenizing the cells, as these structures by their shape, distribution and composition *determine* "bulk" cell permittivity and conductivity. Electro-orientation, coupled with the dipole theory of this paper, provides one means of estimating these parameters with relative ease.

This work would not have been possible without the assistance of several people. Mr. Dan Michalowski, Director, and Dr. Jeff Wyatt, veterinarian, of Seneca Park Zoo, Rochester, NY supplied the llama blood used in this study. Dr. Rick Waugh and his lab supplied the human blood samples. Special thanks to the reviewers for their insightful comments, which helped us clarify our presentation.

The work was supported by grants from the Particulate and Multiphase Processes Program of the National Science Foundation Division of Engineering and from Eastman Kodak Company, as well as the Sproull Fellowship Program of the University of Rochester (R. D. Miller).

Received for publication 27 May 1992 and in final form 21 December 1992.

REFERENCES

1. Teixeira-Pinto, A. A., L. L. Nejelski, Jr., J. L. Cutler, and J. H. Heller. 1960. The behavior of unicellular organisms in an electromagnetic field. *Exp. Cell Res.* 20:548–564.
2. Griffin, J. L. 1970. Orientation of human and avian erythrocytes in radio-frequency fields. *Exp. Cell Res.* 61:113–120.
3. Griffin, J. L., and R. E. Stowell. 1966. Orientation of *Euglena* by radio-frequency fields. *Exp. Cell Res.* 44:684–688.
4. Ascoli, C., M. Barbi, C. Frediani, and D. Petracchi. 1978. Effects of

electromagnetic fields on the motion of *Euglena gracilis*. *Biophys. J.* 24:601–612.

5. Iglesias, F. J., M. C. Lopez, C. Santamaria, and A. Dominguez. 1985. Orientation of *Schizosaccharomyces pombe* non-living cells under alternating uniform and non-uniform electric fields. *Biophys. J.* 48:721–726.
6. Fomchenkov, V. M., and B. K. Gavrilyuk. 1977. Dielectrophoresis of cell suspensions. *Stud. Biophys.* 65:35–46. (in Russian)
7. Fomchenkov, V. M., and B. K. Gavrilyuk. 1978. The study of dielectrophoresis of cells using the optical technique of measuring. *J. Biol. Phys.* 6:29–68.
8. Schwarz, G., M. Saito, and H. P. Schwan. 1965. On the orientation of nonspherical particles in an alternating electric field. *J. Chem. Phys.* 43:3562–3569.
9. Saito, M., H. P. Schwan, and G. Schwarz. 1966. Response of nonspherical biological particles to alternating electric fields. *Biophys. J.* 6:313–327.
10. Schwan, H. P. 1957. Electrical properties of tissue and cell suspensions. *Adv. in Biol. Med. Phys.* 5:148–209.
11. Ferris, C. D., and J. L. Griffin. 1977. Orientation of *Euglena gracilis* by electromagnetic fields: theory and experiment. *Acta Biol. Acad. Sci. Hung.* 28:375–387.
12. Landau, L. D., and E. M. Lifshitz. 1984. Electrodynamics of Continuous Media, 2nd ed. Pergamon Press, Oxford. 460 pp.
13. Sauer, F. A. 1983. Forces on suspended particles in the electromagnetic field. *In* Coherent Excitations in Biological Systems. H. Frölich and F. Kremer, editors. Springer-Verlag, Berlin. 134–144.
14. Gruzdev, A. D. 1965. Orientation of microscopic particles in electric fields. *Engl. Transl. Biofizika.* 10:1206–1208.
15. Fomchenkov, V. M., A. L. Mazanov, and V. N. Brezgunov. 1982. Effect of dispersion of electrical parameters of bacterial cells on their orientation in an alternating electric field. *Engl. Transl. Biofizika.* 27:692–697.
16. Fåhraeus, R. 1929. The suspension stability of blood. *Physiol. Rev.* 9:241–274.
17. Rowlands, S., and L. Skibo. 1972. The morphology of red-cell aggregates. *Thromb. Res.* 1:47–58.
18. Rowlands, S. 1983. Coherent excitations in blood. *In* Coherent Excitations in Biological Systems, H. Fröhlich and F. Kremer, editors. Springer-Verlag, Berlin. 145–161.
19. Holzapfel, C., J. Vienken, and U. Zimmermann. 1982. Rotation of cells in an alternating electric field: theory and experimental proof. *J. Membr. Biol.* 67:13–26.
20. Miller, R. D., and T. B. Jones. 1987. Frequency-dependent orientation of ellipsoidal particles in ac electric fields. *In* Proc. Ninth Annu. Conf. IEEE Engineering in Medicine and Biology Society, Boston, November 1978. pp. 710–711.
21. Asami, K., T. Hanai, and N. Koizumi. 1980. Dielectric approach to suspensions of ellipsoidal particles covered with a shell, in particular reference to biological cells. *Japanese J. Appl. Phys.* 19:359–365.
22. Stepin, L. D. 1965. Dielectric permeability of a medium with nonuniform ellipsoidal inclusions. *Soviet Physics—Technical Physics.* 10:768–772. (Engl. Trans. *Zhurnal Tekhnicheskoi Fiziki* 35:996–1001.)
23. Stratton, J. A. 1941. Electromagnetic Theory. McGraw Hill, NY. 615 pp.
24. Pauly, H., and H. P. Schwan. 1966. Dielectric properties and ion mobility in erythrocytes. *Biophys. J.* 6:621–639.
25. Cole, K. S. 1935. Electric impedance of *Hipponoë* eggs. *J. Gen. Physiol.* 18:877–887.
26. Fricke, H. 1953. Relation of the permittivity of biological cell suspensions to fractional cell volume. *Nature (Lond.).* 172:731–732.
27. Fricke, H., H. P. Schwan, K. Li, and V. Bryson. 1956. A dielectric study of the low-conductance surface membrane in *E. coli*. *Nature (Lond.).* 177:134–135.
28. Buetow, D. E. 1968. The morphology and ultrastructure of *Euglena*. *In* The Biology of *Euglena*. Vol. I. Academic Press, New York. 110–184.
29. Zimmerman, U., and J. Vienken. 1982. Electric field-induced cell-to-cell fusion. *J. Membr. Biol.* 67:165–182.
30. Zimmerman, U., J. Vienken, and G. Pilwat. 1984. Electrofusion of cells. *In* Investigative Microtechniques in Medicine and Biology, Vol. I. J. Chayen and L. Bitensky, editors. Marcel Dekker, Inc., New York. 89–167.